DE-FG07-99ER62889

FINAL REPORT

Fate and Transport of Radionuclides Beneath the Hanford Tank Farms: Unraveling Coupled Geochemical and Hydrological Processes in the Vadose Zone

Introduction

Although the accelerated transport of ^{99}Tc, ^{137}Cs, and ^{235}U within the vadose zone beneath the 200-West Area of the Hanford tank-farm area has been recognized, the mechanisms responsible for the vertical migration of the radionuclides is unclear. Does horizontal stratification enchance the lateral movement of contaminants, which in turn enhances vertical perferential flow due to perched water dynamics? Do physical heterogeneties, such as stratification and pore regime connectivity, influence the retardation and degree of geochemical nonequilibrium during contaminant transport? Recent modeling efforts of the problem have failed to yield answers to this question since they are inadequately parameterized due to the lack of sufficient quality data. Fundamental experimental research is needed that will improve the conceptual understanding and predictive capability of radionuclide migration in the Hanford tank-farm environment. Since geochemical reactions are directly linked to the system hydrodynamics, coupled geochemical and hydrological processes must be investigated in order to resolve the key mechanisms contributing to vadose zone and groundwater contamination at Hanford.

Our research group has performed extensive investigations on time-dependent contaminant interactions with subsurface media using dynamic flow techniques which more closely simulate conditions in-situ. Of particular relevance to this proposal is the work of Barnett et al. (2000) who showed that U(VI) transport through Hanford sediments was highly retarded and extremely sensitive to changes in pH and total carbonate. What remains elusive are the geochemical mechanisms for uranium retention—necessary information for accurately simulating transport—and are thus the focus of this study. The experimental and numerical results from this research will provide knowledge and information in previously unexplored areas of vadose zone fate and transport to support EM's performance/risk assessment and decision-making process for Tank Farm restoration. By unraveling fundamental contaminant transport mechanisms in complex porous media, we provide an improved conceptual understanding and predictive capability of a variety of vadose issues within the DOE system.

Progress and Relevance to EM Needs

Detailed investigations of uranyl sorption have been performed for a range of soil solids. Iron (hydr)oxides including ferrihydrite, goethite, and hematite sorb uranium(VI)

strongly under neutral to slightly basic conditions. Dissolved carbonate complexes form under strongly alkaline conditions, leading to desorption of uranium. A variety of surface complexes have been postulated, although recent spectroscopic data suggests that uranium carbonate ternary complexes may be the principal surface species.

Mechanistic investigations of uranyl sorption on heterogeneous soils and sediment are complicated by the presence of multiple minerals, biological activity, and organic matter. In these systems, the chemical and microbial processes can reduce uranium to form insoluble U(IV) and mixed-valence oxides. Uranyl precipitates including uranyl phosphates, hydroxides, and carbonates can form in oxic, highly contaminated soils and sediments. Under aerated soil conditions and neutral or higher pH, uranyl carbonate complexes dominate and limit sorption.

Uranyl surface species and their sorption mechanism have largely been determined through surface complexation modeling; direct identification of uranium surface complexes on soils and sediments has been less common. Accurately determining the surface structure of U is vital to determine the fate of this hazardous element in the environment. Strong sorption complexes and surface precipitates are the least labile and thereby decrease uranium bioavailability and transport. X-ray absorption spectroscopy (XAS) provides an *in-situ*, element-specific probe of the local structure of the surface complex, and with it the principal sorption mechanisms. Accordingly, in this study we used XAS to determine the sorption mechanism of uranyl on several soils and sediments that are associated with uranium contamination. A detailed understanding of the sorption mechanism will provide insight into its stability, and thus its transport and bioavailability. It will also help to determine the principal soil minerals that control uranium sorption.

Experimental Approach

Sample Description

Subsurface media from three U.S. Department of Energy facilities, including the Oak Ridge (OR) Reservation in Tennessee, the Savannah River (SR) site in South Carolina, and the Hanford (HF) Nuclear Reservation in Washington were used in this study. All three sites have a legacy of U waste disposal and subsurface contamination. The OR soil was taken from a C-horizon (1.5 m depth) of an Inceptisol with a shale-limestone parent material that has weathered into acidic clay-rich deposits. Sediments from the SR site are from the McBean formation and were taken from a depth of 45 m. The SR sediments are acidic with similar clay content to the OR soil. HF subsurface media were acquired from shallow (1 m) depths in the Upper Ringold Formation. Unweathered sand particles comprise the bulk of the HF media. Iron oxides coat much of the mineral surfaces in each of the media and may thus control surface reactivity.

Uranium was sorbed to the media using both batch and column reactors as described by Barnett et al. (2000). Batch experiments were conducted by placing 0.1 g solid phase in 30 mL 0.01 M $NaNO_3$. The pH was then adjusted between 4 and 6 using 0.1 N HNO_3 and NaOH. Uranium(VI) was added to this suspension to create a solution with 21.3 μmol L^{-1} or 42.6 μmol L^{-1} (5 or 10 mg/L) total U. The samples were saturated with air to ensure carbonate equilibrium, and the reaction was allowed to proceed for approximately 48 hours. The suspensions were filtered and the residual solution U quantified using a kinetic phosphorescence analyzer. Adsorbed U was inferred by difference between initial and final U concentrations. The solids were packed into a 5 x 5 x 30 mm polycarbonate sample holder and sealed with Kapton film for analysis. Media reacted with U in transport columns were also studied. A 1-cm diameter

by 1.7-cm long column was packed with solids. These columns were then equilibrated with 0.01 M $NaNO_3$. Uranium was then added to this solution (5 mg L^{-1} net concentration) and passed through the column at a flow rate of 4.3 cm h^{-1}. The uranium content of the effluent was monitored and sorption was determined by difference between the integrated input uranium concentration and the output uranium concentration. Once appreciable sorption was achieved, the solids were removed from the column and placed in a polycarbonate sample holder for x-ray absorption spectroscopic analysis.

XAS Spectroscopy

X-ray absorption spectroscopy (XAS) was performed at the Stanford Synchrotron Radiation Laboratory on beamlines 4-2 or 4-3. The storage ring operated at 3.0 GeV and at currents between 50 and 100 mA. Spectra were taken with a Si(220) double-crystal monochromator with an unfocused beam. Incident and transmitted intensities were measured with 15-cm N_2-filled ionization chambers. Sample fluorescence was measured with a multi-element Ge detector oriented 45 degrees off the sample and orthogonal to the incident radiation. The beam was detuned approximately 50% to reject higher-order harmonic frequencies and to prevent detector saturation.

X-ray absorption spectra were collected from –200 to +1000 eV about the L_{III}-edge of U (17,166 eV). At least 5 spectra were collected for each sample and averaged for analysis. Internal calibration was achieved with uranyl nitrate between the second and third ionization chambers; its inflection point was set at 17176 eV.

Data Analysis

XANES Spectroscopy: The x-ray absorption near-edge structure (XANES) spectra were analyzed using Peak Fit 4.0 (Jandel Scientific) and WinXAS (Ressler, 1997). The background was subtracted and the jump height normalized to unity for comparison. No smoothing of the raw spectra was done to preserve spectral line-shapes. These spectra were fit using linear combinations of U(IV) and U(VI), as UO_2 and uranyl nitrate standards, respectively. The fractions of each species in the fit were used to determine the oxidation state of the uranium in the subsurface media. Fits were verified to be accurate within 4% by quantifying the fractions of U(IV) and U(VI) in a series of mixtures of known composition. The fitting is based on the shift in binding energy of the U L_{III}-shell (2p orbital) as a function of oxidation state. The higher oxidation state, U(VI), has a larger effective nuclear charge and thus has a slightly higher binding energy. First-derivative fits are more sensitive to the edge position and consequently were also used in spectral comparisons. Smoothed (3% Savitsky-Golay smoothing) first-derivative XANES spectra were then fit using linear combinations of the first-derivative U(IV) and U(VI) standard spectra similar to the method used for the raw spectra.

EXAFS Spectroscopy: Following spectral averaging, the background was subtracted from the spectra using a polynomial fit the resulting spectral jump heights normalized to unity. A six-point cubic spline function that followed the envelope of the decaying spectrum was used to isolate the EXAFS spectral contribution (the $\chi(k)$ function). The energy (eV) scale was transformed to k-range using 17,166 eV as the energy of the U L_{III} edge (E_0). The $\chi(k)$ spectrum was then weighted by k^2 in order to amplify the upper k-range and Fourier-transformed without smoothing to produce a radial structure function (RSF) using a k-range of approximately 3 to 15 $Å^{-1}$. Distinct shells of the RSF function were then back-transformed to isolate the spectral contributions of each atomic shell. Final fits were completed using unfiltered k-weighted $\chi(k)$ spectra.

The WinXAS software package was used for EXAFS data analysis using phase and amplitude functions derived using FEFF 7.02. Single and multiple scattering paths were considered, although no multiple scattering paths were required for fitting. The accuracy of these phase and amplitude functions were confirmed by comparing fits of uranyl nitrate, uranium(IV) oxide, and uranium(VI) oxide with known structures. Phase and amplitude functions calculated using FEFF were also similar to those extracted from the spectra of known standards.

The type (Z), coordination number (CN), distance (R), and the Debye-Waller factor (σ^2) of the atoms coordinating U were determined by fitting the experimental spectrum. The Debye-Waller factor is

effectively the variance in the bond length, and is a measure of the disorder of the coordination environment. Each variable was independently varied except E_0 and σ^2. E_0 was constrained to the same value for each shell. Fitting did not appreciably change the values of σ^2; thus, σ^2 was constrained to minimize the number of variables required for fitting. The Debye-Waller factor was set to 0.002 for the axial oxygens and 0.005 for other shells while the CN was varied; these values were selected based on $(UO_2)(CO_3)_3^{4-}$ solutions. For OR samples, the equatorial oxygens had greater disorder, thus σ^2 was varied in the fitting of this shell. Once the filtered spectra were fit, the resulting parameters were combined and refit to the unfiltered $\chi(k)$ spectrum. The accuracy of the fits was estimated using the χ^2 statistical parameter, for which smaller values correspond to the best fits. Each fit had a reduced χ^2 of about 6000 for unsmoothed $k^2\chi(k)$ spectra, and approximately 420 using RSF's. By comparison with model compounds, the interatomic distances can be determined within 0.02 Å and the coordination number within 30% for the first shell and less accurate for more distant shells. Elements of similar atomic number ($Z\pm1$) cannot be distinguished due to similarities in the phase and amplitude functions, although differences in local structure (i.e. interatomic distances) may help to determine more information about which element is present.

Experimental Results and Relevance

Transport Studies

Batch and flow studies correlate the adsorption of U(VI) under static and dynamic conditions. For each of the subsurface media, uranium sorption was non-linear and modeled with a Freundlich isotherm, suggesting that the free energy of sorption decreases as the surface loading increases. Sorption was appreciable between approximately pH 4.5 and 8.5. Uranium solution concentration influenced the sorption envelope position. Magnesium, calcium, and dissolved silica competitively inhibited U(VI) retention, suggesting that at least some of the U was bound to exchangeable adsorption sites.

In hydrodynamic experiments, solids sorbed significantly more U than predicted by batch experiments alone, although sorption was reversible and uranium was completely recoverable. As a result, batch-derived transport parameters significantly overestimated uranium flux through the soil columns. The HF medium retarded uranium transport nearly twice as much as OR and SR media. Uranium transport was asymmetric, due to nonlinear adsorption, multiple adsorption sites, and kinetic factors. These data suggest that there were multiple site-types of different reactivity, and complex kinetic factors that influenced sorption. Reversible U(VI) sorption in batch and column studies implied outer-sphere sorption. However, the extensive partitioning of U(VI) to the solid phase suggests that some of uranium may be bound at least in part as an inner-sphere complex. However, if inner-sphere complexes form they must be relatively labile to describe the reversible sorption observed in both in batch and flow experiments.

The similarity in uranyl sorption to each of the media as a function of pH suggests the possibility of common sorption mechanisms within each. Iron content, which is near 25 g kg^{-1} for each medium, may be responsible for the similar adsorption properties. For HF media, the majority of the reactive surface area is attributed to iron oxides. SR and OR media contain significant clay minerals that could also sorb U; however, the presence of these clays does not significantly increase U sorption relative to the clay deficient HF media. Organic matter and Mn oxide content are variable for the three media and do not

correlate with uranyl sorption. XAS was used to help resolve the importance of each sorption mechanism of U in these media.

Oxidation State

XANES spectroscopy was used to determine the oxidation state and coordination environment of uranium in each subsurface media. The U-L_{III} XANES spectra of OR, SR, and HF media each have an absorption edge at 11876 eV (Fig. 1). Additionally, the spectra have comparable features to those of uranyl nitrate, suggesting uranium is present as the uranyl ion. Fitting the spectra with model compounds also indicates the dominance of U(VI).

Derivative spectra can detect small fractions of U(IV) that may be present in the samples but not visible in the raw spectra. For the first-derivative spectra, a single primary peak corresponding to the absorption edge is noted, suggesting the presence of a single oxidation state. The absorption edge occurred near 11876 eV for each of the subsurface media (Fig. 2), confirming that uranium is present primarily as U(VI). Fitting of these spectra also required no contributions from U(IV) species, further indicating that only minor fractions, if any, of the uranium is reduced during batch or transport experiments. Therefore, uranium reduction to insoluble UO_2(s) does not explain the increased sorption capacity of the soils in column experiments—as would be expected based on the reversibility of sorption.

XANES spectroscopy also yields structural information resulting from multiple scattering contributions and electronic transitions. The U-L_{III} XANES spectra each contain similar fine structure in the region immediately following the edge, implying that similar species are sorbed to each of the media. Furthermore, the XANES spectra correspond well with the spectrum of uranyl nitrate, suggesting a uranyl-type coordination environment. The prevalence of the uranyl cation is not surprising since it is the most stable under oxidizing conditions that were used in these transport studies.

Local Structure

EXAFS spectroscopy is useful for determining the average local structure of uranium sorbed to subsurface media. The EXAFS spectra of hydrated uranyl cations contain three principal shells. The first shell is characteristic of the axial oxygens of the uranyl cation, and the second shell corresponds to the oxygens from water and other ligands in the equatorial plane. The second shell may also contain contributions from second-nearest neighbor ligands such nitrate, carbonate or carboxylate. More distant neighboring atoms also form a third coordination shell.

The EXAFS spectra for the reacted media show the presence of a large first shell and at least two other shells (Fig. 3). Figure 4 contains a deconvolution of the fit using OR4 as an example. The first shell corresponds to approximately 2 oxygens at a distance of 1.78 Å, d(U-O_{ax}), similar to that reported for other UO_2^{2+} species. Furthermore, the axial oxygen coordination environment of uranyl is not altered appreciably when sorbed (see, for example, Waite et al., 1994; Chisholm-Brause et al., 1994, Hudson et al. 1999)

or incorporated into solids (e.g., Mercier et al., 1995; Allan et al., 1996, Reeder et al., 2000); thus, changes in the axial coordination environment are not expected.

The U-O coordination environment of the equatorial oxygens has considerable disorder. Two U-O_{eq} coordination shells were distinguished, the first at a distance of approximately 2.30 Å and the second at a somewhat longer distance, 2.42 Å. For HF1 and SR1, both equatorial O distances were fit with similar coordination numbers. However, OR soils exhibit larger coordination numbers and disorder for the U-O_{eq} shell at 2.41 Å. These coordination environments imply that two distinct species coordinate the uranyl cation in the equatorial plane, and that the quantity of these species is comparable for HF1 and SR1 media, while one species is more significant for the OR soil.

Uranium sorption on these subsurface media is reversible under hydrodynamic conditions (Barnett et al., 2000), similar to labile outer-sphere surface complexes. And outer-sphere sorption of the fully hydrated cation is appreciable on clay minerals (Chisholm-Brause et al., 1994, Hudson et al. 1999). However, outer-sphere complexes are symmetric with a single U-O distance for equatorial oxygen at about 2.43 Å. The presence of two distinct d(U-O_{eq}) signifies that formation of fully-hydrated outer-sphere complexes is not the only mechanism of sorption.

The split in the equatorial oxygen shells futher implies that ligands other than water are present in the equatorial plane. Chemically bound ligands disrupt the equatorial waters, and result in the formation of an elongated U-O_{ligand} distance and shortened equatorial U-O_{H2O} distance. For example, uranyl nitrate hexahydrate contains two bidentate nitrate groups with a d(U-O_{NO3}) of 2.52 Å, while equatorial waters have contracted uranium-oxygen distances of about 2.39 Å (Table 2, Fig. 3). Similar variation in the coordination environments of equatorial oxygen are found for uranyl carbonate (Bargar et al., 1999) and uranyl phosphate (Mercier et al., 1985) complexes.

Several structural models explain the presence of a split equatorial oxygen shell. Surface hydroxyls of many soil minerals could form inner-sphere complexes with the uranyl cation, with longer bonds to the surface bridging oxygens and shorter U-O bonds to the residual waters. Such inner-sphere complexes form on ferrihydrite (Waite et al., 1994) and could similarly form on other surface hydroxyl sites such as aluminol or silanol groups (Hudson et al. 1999). Recent evidence suggests that uranium sorption may form inner-sphere ternary surface complexes (Bargar et al., 1999) and even polymeric species (Waite et al., 1994; Hudson et al., 1999) coordinated to both a surface and a ligand.

Examination of more distant neighbors provides a means to determine which surface complexes are most significant under the conditions of this study. For HF1, an additional spectral feature is present as a high-distant shoulder to the equatorial oxygen in the FT spectrum (Fig. 3). We fit this spectral feature with 1 C atom at 2.89 Å, similar to carbonate ternary surface complexes proposed for uranyl sorption on iron oxides (Barger et al., 1999). The structural environments for other bidentate carbonate complexes also have a similar d(U-C) and split in the equatorial oxygen shell. A U-Fe shell with a distance of about 3.42 Å is also present, similar to that of uranyl carbonate ternary complexes on ferrihydrite (Bargar et al., 1999). Thus, EXAFS data suggest that uranyl carbonate complexes form on iron (hydr)oxides for HF1.

In contrast, a clear spectral feature in the FT spectra is noted at a distance (uncorrected for phase shift) of 3.1 Å of SR and OR solids (Figs. 3 and 4). This feature is best described with a U-P shell at a distance of 3.61 Å (Fig. 5, Table 4). The U-P distance correlates with other bidentate mononuclear complexes (Table 2, Mercier et al., 1985) and for uranyl adsorbed on phosphate minerals (Drot et al., 1998). Multiple scattering (MS) may also contribute to the feature observed in the uncorrected FT spectra of OR and SR media at 3.1 Å (Fig. 5). This is an unlikely result in the present system, however, since highly symmetric rather than disordered structural environments contribute to MS features (Thompson et al., 1997).

Uranyl incorporation into discrete solid phases or on phosphate surface groups (including those resulting from phosphate sorption to iron oxides) may explain the existence of a U-P shell at 3.6 Å (Arey et al., 1999). Uranyl sorbed on phosphate solids (Drot and Simoni, 1999, Drot et al., 1999) and secondary uranyl phosphates (e.g., Burns, 1999) both contain U-P distances comparable to those determined here. Precipitation of insoluble uranyl phosphates, however, is a slow, irreversible, process incompatible with the reversible adsorption observed for these subsurface media (Barnett et al., 2000). Aqueous uranyl phosphate complexes commonly formed in solutions having PO_4^{3-}:CO_3^{2-} ratios greater than 10 (Sandino and Bruno, 1992; Brendler et al., 1996) and may be similar to the surface complexes in these studies.

While it appears that uranium in SR and OR media is present as a phosphate complex based on spectral data, it is unclear if adequate P is present in subsurface media to account for the extent of uranium sorption. The low U-P coordination number, typically only about 0.5, indicates that only a fraction of adsorbed uranium is complexed to phosphate. Hence, other uranyl surface complexes, including those directly on iron (hydr)oxides or clay minerals, are also likely to be present. EXAFS cannot distinguish between P, Si, or Al; it is thus possible that U-Al or U-Si contributions explain a portion of the observed U-P shell in OR and SR media. A bidentate, mononuclear surface complex formed on aluminosilicate clay minerals would result in a *d*(U-Si/Al) between 3.4 and 3.7 Å, similar to the measured *d*(U-P). EXAFS spectral features attributed to Si or Al have rarely been observed for inner-sphere uranyl complexes on clay minerals (Chisholm-Brause et al. 1994; Hudson et al., 1999; Sylwester et al., 2000); however, Moyes et al. (2000) detected *d*(U-Si) at both 2.75 Å (to Si) and 3.66 Å (to Al). While the 3.66 Å peak may be observed in our data, the U-Si peak at 2.75 Å is absent. Additionally, inner-sphere uranyl complexes on silica contain shorter U-Si distances, 3.2 Å (Sylwester et al., 2000), compared to the 3.6 Å distance observed in these experiments. Therefore, it is unlikely that Al and Si backscattering features alone describe the U-P shell. The lack of Al and Si spectral features does not preclude the presence of inner-sphere sorption to clay minerals, but the extent of sorption is less than our detection limits.

Similarities in the sorption behavior of uranyl within each medium suggest a common phase may be important in retention; iron (hydr)oxides fit this criterion, having similar concentrations within each medium and also having a known affinity for uranyl (Barnett et al., 2000). EXAFS data partially supports this hypothesis in that the addition of an iron shell improved the fits for the filtered spectra of all subsurface media examined (Fig. 5). However, spectral fitting also required a U-P shell in each case and the U-Fe shell is insignificant when fitting was performed on the raw, unfiltered spectra.

Therefore, the iron shell is not conclusive and is not included in the final fits of the raw spectrum.

Both inner- and outer-sphere ternary uranyl complexes may be associated with iron (hydr)oxides and aluminosilicates (Fig. 6). Additionally, phosphate may be a surface ligand on the iron (hydr)oxide. The association of ternary uranyl carbonates with iron (hydr)oxides is also suggested by previous research (Waite et al., 1994; Duff and Amrhein, 1996; Bargar et al. 1999). In heterogeneous soil matrices, it is likely that a mixture of sorption complexes is present. However, the reversibility of uranyl sorption indicates that any inner-sphere complexes are relatively labile. The low coordination numbers suggests that these inner-sphere complexes represent only a portion of the sorbed uranium. It should be noted, however, that constrained Debye-Waller factors may further reduce the calculated coordination numbers relative to the actual value (i.e., the reported values are very conservative estimates and are likely much lower than the actual values). Additional complexes are likely present but not detected due to disorder or destructive interference.

Under no conditions are U-U features visible in the spectra of the subsurface media. Therefore, neither polynuclear nor uranyl solids such as schoepite are an appreciable fraction of the sorbed uranium. The equilibrium sorption pH varied between 4.04 and 6.55 for SR1 and OR3, and schoepite and rutherfordine (UO_2CO_3) are thus undersaturated. At pH 4, the predominant solution species are UO_2^{2+} and $UO_2(OH)^+$, while the major uranyl species in an air-saturated system at pH 6.5 are $(UO_2)_3(OH)_5^+$, $UO_2(OH)^+$ and $UO_2CO_3^0$ (Grenthe et al., 1992; Shock et al., 1997). Despite the stability of multinuclear solution complexes in OR3 and OR4 (pH 6.55 and 5.72 respectively), they did not comprise a significant fraction of sorbed uranium—consistent with the surface complexation modeling of Waite et al. (1994).

Residence-Time Effects

The effects of equilibration time was studied by examining the conditions under which UO_2^{2+} is sorbed on OR soils. Samples OR1 and OR3 were loaded with U(VI) in batch experiments equilibrated for 48 h to allow for near steady-state sorption. HF1, SR1, OR2 and OR4, were reacted under hydrodynamic conditions with hydraulic residence times of only 0.18 h. Consequently, the transport models of Barnett et al. (2000) require different partitioning coefficients for column and batch studies. Furthermore, the models that were used to describe transport phenomena indicate kinetic limitations in uranyl sorption. While these factors suggest that different sorption mechanisms may be operational in each system, the spectra exhibit no significant differences that can be attributed to the method of loading.

Conclusions

Hydrodynamic experiments demonstrate that uranyl is relatively labile—uranium sorption on these materials is reversible consistent with outer-sphere sorption mechanisms. However, spectroscopic examination reveals disordered inner-sphere complexes that are most likely in conjunction with outer-sphere complexes and combine to provide the noted lability. Interestingly, the local structure of uranyl varied little

between the different subsurface media, suggesting similar complexes were present in each. Most noteworthy, ternary uranyl complexes are appreciable surface species under the conditions of this study. The SR and OR subsurface media contained uranyl phosphate complexes, while U in the HF media is retained as carbonate species.

Literature Cited

Allan, P.G., D. K. Shuh, J. J. Bucher, N. M. Edelstein, C. E. A. Palmer, R. J. Silva, S. N. Nguyen, L. N. Marquez and E. A. Hudson. 1996. Determinations of uranium structures using EXAFS: schoepite and other U(VI) oxide precipitates. *Radiochim. Acta* **75**:47-53.

Arey, J. S., J. C. Seaman and P. M. Bertsch. 1999. Immobilization of uranium in contaminated sediments by hydroxyapatite addition. *Environ. Sci. Technol.* **33**:337-342.

Bargar, J. R. Reitmeyer and J. A. Davis. 1999. Spectroscopic confirmation of uranium(VI)-carbonato adsorption complexes on hematite. *Environ. Sci. Technol.* **33**:2481-2484.

Barnett, M. O., P. M. Jardine, S. C. Brooks and H. M. Selim. 2000. Adsorption and transport of U(VI) in subsurface media. *Soil Sci. Soc. Am. J.*, 64:908-917.

Brendler V., G. Geipel, G. Bernhard and H. Nitsche. 1996. Complexation in the system $UO_2^{2+}/PO_4^{3-}/OH^-$ (aq): potentiometric and spectroscopic investigations at very low ionic strength. *Radiochim. Acta.* **74**:75-80.

Burns P.C. 1999. The crystal chemistry of uranium, pp 23-90. *In* P. C. Burnes and R. Finch (ed.) Uranium: mineralogy, geochemistry, and the environment. Vol. 38, Reviews in Mineralogy, Mineralogical Society of America, Washington D.C.

Chisholm-Brause, C., S. D. Conradson, C. T. Buscher, P. G. Eller and D. E. Morris. 1994. Speciation of uranyl sorbed at multiple binding sites on montmorillonite. *Geochim. Cosmochim. Acta* **58**:3625-3621.

Drot R., E. Simoni, M. Alnot and J. J. Ehrhardt. 1998. Structural environment of uranium(VI) and europium(III) species sorbed onto phosphate surfaces:XPS and optical spectroscopy studies. *J. Colloid Interface Sci.* **205**:410-416.

Drot, R. and E. Simoni. 1999. Uranium(VI) and europium(III) speciation at the phosphate compounds solution interface. *Langmuir* **15**: 4820-4827.

Drot, R., E. Simoni and C. Denauwer. 1999. Structural environment of uranium(VI) species sorbed onto ZrP2O7:x-ray absorption spectroscopy study. *Comptes Rendus De L'Academie Des Sciences Serie II Fascicule C-Chimie* **2**:111-117.

Duff, M. C. and C. Amrhein. 1996. Uranium(VI) adsorption on goethite and soil in carbonate solutions. *Soil Sci. Soc. Am. J.* **60**:1393-1400.

Hudson, E. A., L. J. Terminello, B. E. Viani, M. Denecke, T. Reich, P. A. Allen, J. J. Bucher, D. K. Shuh and N. M. Edelstein. (1999) The structure of U^{6+} sorption complexes on vermiculite and hydrobiotite. *Clays Clay Min.***47**:439-457.

Mercier, R., M. Phoem-Thi and P. Coomban. 1985. Structure, vibrational study, and conductivity of trihydrated uranyl bisdihydrogen phosphate:$UO_2(H_2PO_4)_2{\cdot}3H_2O$. *Solid State Ionics* **15**:113-126.

Moyes, L. N., R. H. Parkman, J. M. Charnock, D. J. Vaughan, F. R. Livens, C. R. Hughes and A. Braithwaite. 2000. Uranium uptake from aqueous solution by interaction with goethite, lepidocrosite, muscovite, and mackinawite: an x-ray absorption spectroscopy study. *Environ. Sci. Technol.* **34**:1062-1068.

Reeder, R.J., M. Nugent, G. M. Lamble, C. D. Tait, and D. E. Morris. 2000. Uranyl incorporation into calcite and aragonite: XAFS and luminescence studies. *Environ. Sci. Technol.* **34**:638-644.

Ressler, T. 1997. WinXAS: A new software package not only for the analysis of energy-dispersive XAS data. *J. Physique IV* **7**:269-C270.

Sandino, A. and J. Bruno. 1992. The solubility of $UO_2)_3(PO_4)_2{\cdot}4H_2O$ and the formation of U(VI) phosphate complexes: their influence in uranium speciation in natural waters. *Geochim. Cosmochim. Acta* **56**:4135-4145.

Sylwester, E. R., E. A. Hudson and P. G. Allen. 2000. The structure of uranium (VI) sorption complexes on silica, alumina, and montmorillonite. *Geochim. Cosmochim. Acta* **64**:2431-2438.

Thompson, H.A., G.E. Brown, Jr. and G.A. Parks. 1997. XAFS spectroscopic study of uranyl coordination in solids and aqueous solution. *Am. Mineral.* **82**:483-496.

Waite, T.D., J.A. Davis, T.E. Payne, G.A. Waychunas, and N. Xu. 1994. Uranium(VI) adsorption to ferrihydrite: application of a surface complexation model. *Geochim. Cosmochim. Acta* **58**:5465-5478.

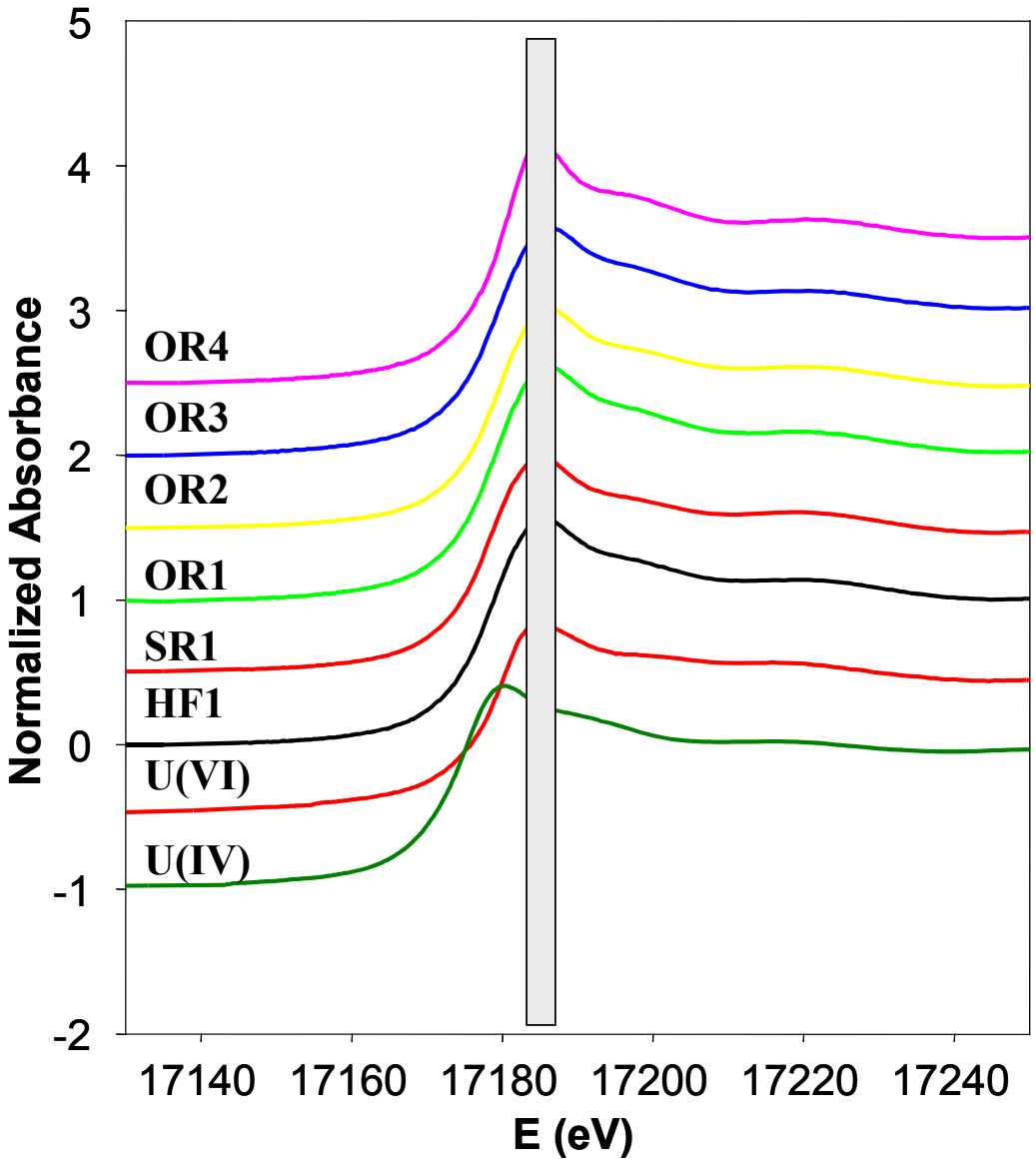

Figure 1. XANES spectra of OR, SR, and HF media compared with the spectra of UO_2 and $UO_2(NO_3)_2 \bullet 6H_2O$.

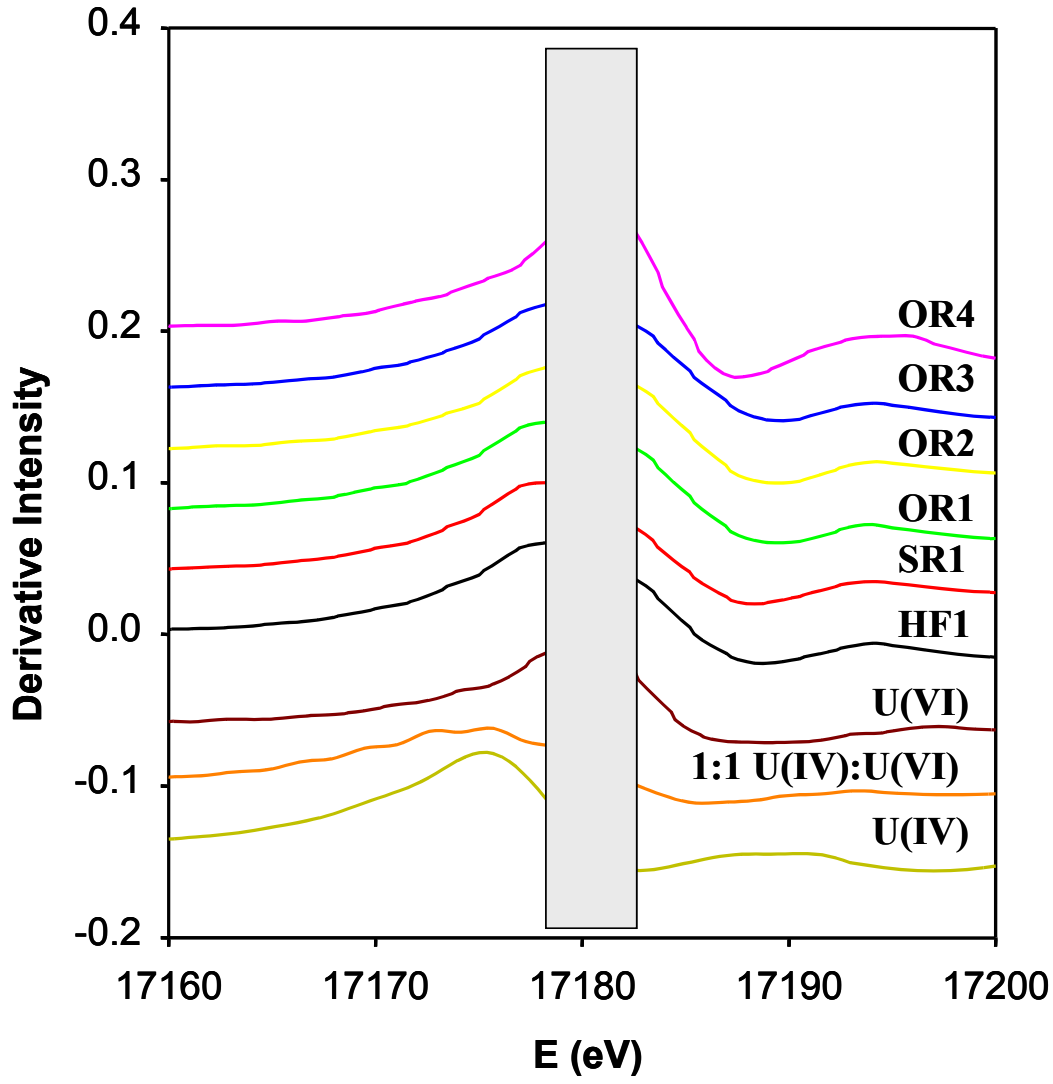

Figure 2. First-derivative XANES spectra of OR, SR, and HF media compared with standards.

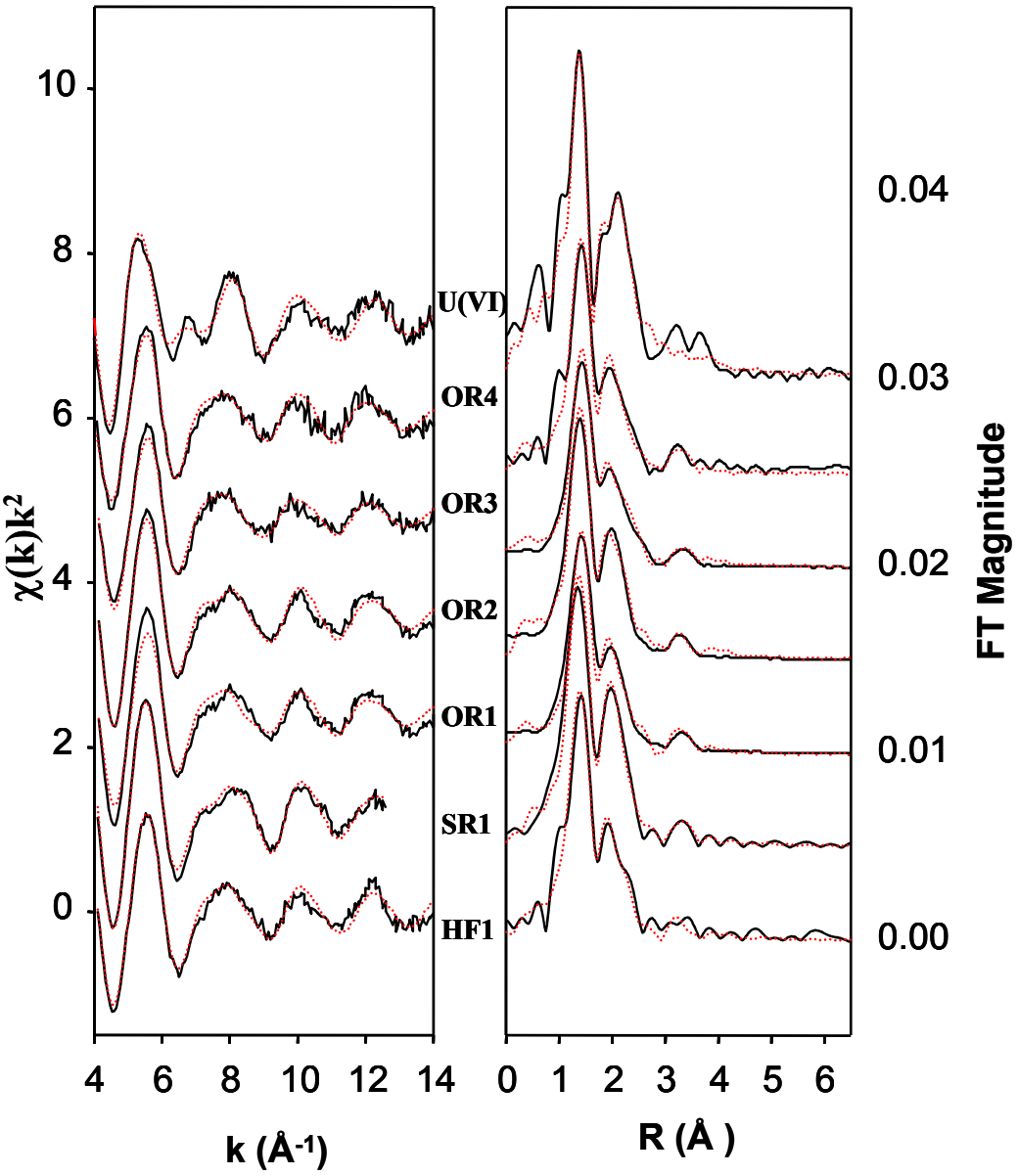

Figure 3. (A) The k^2-weighted $\chi(k)$ U-L_{III} EXAFS spectra and (B) uncorrected radial structure functions for HF, SR, and OR subsurface media sorbed with U. The experimental data (solids lines) are fit (dotted lines) using the parameters described in Table 3.

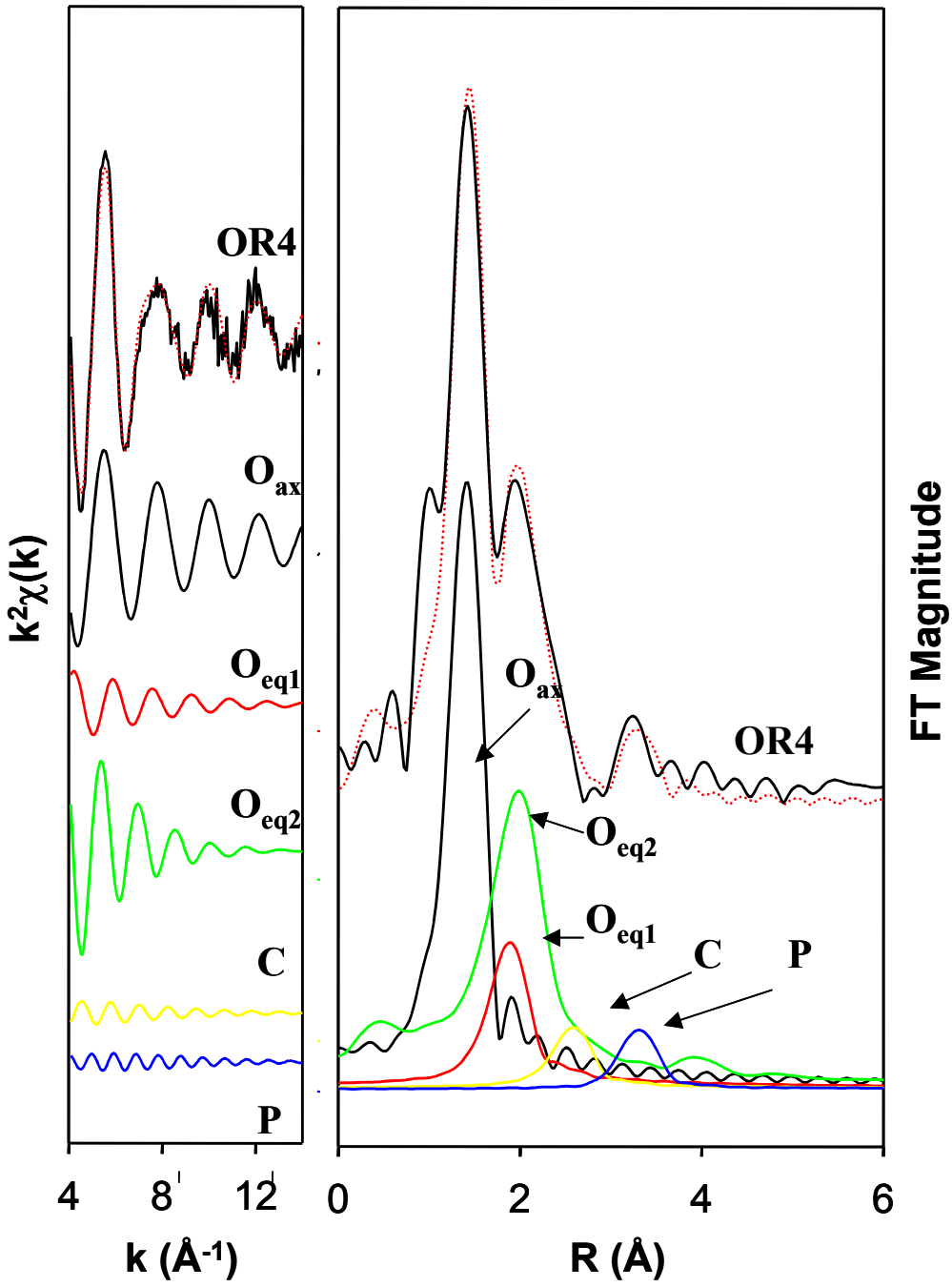

Figure 4. Deconvolution of the $k^2\chi(k)$ spectra (A) and RSF's (B) for OR4. All samples exhibit similar coordination to oxygen. Three U-O distances and a U-P backscatter are required to fit (dotted lines) the experimental spectra (solid lines). A U-C shell is also shown that is only statistically significant for HF1.

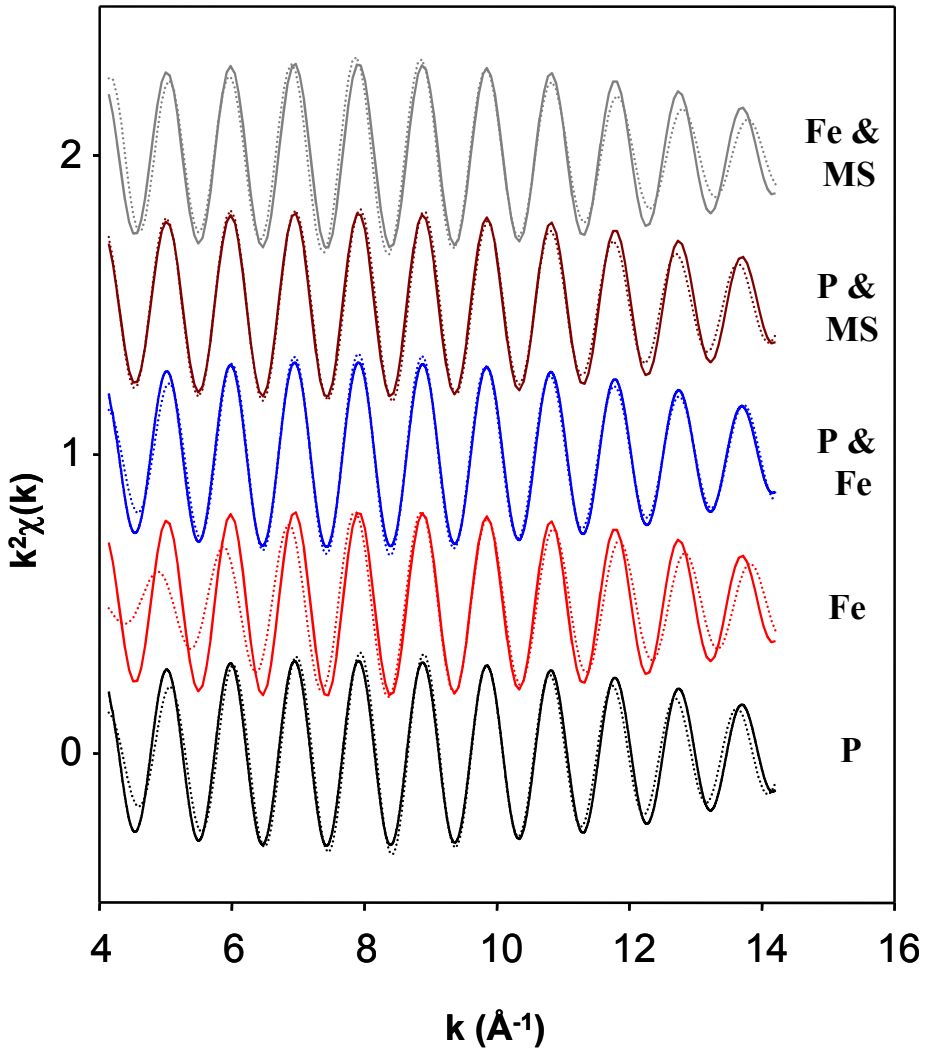

Figure 5. Third-shell (centered at ~3.1 Å) Fourier-filtered EXAFS spectra of OR1. A U-P shell is required for fitting. A U-Fe shell alone is not able to fit the data, although incorporation of a U-Fe contribution with the U-P shell does improve the fit.

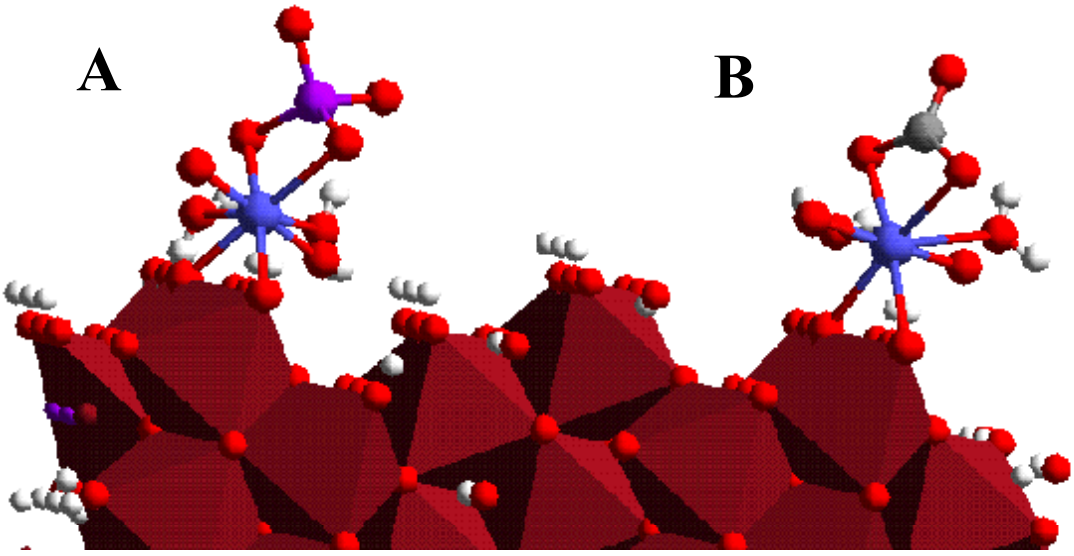

Figure 6. Structural model of U sorbed (A) to SR and OR and (B) to HF subsurface media, showing the formation of an inner-sphere ternary complex containing carbonate for the HF media and phosphate for the OR and SR media. The (110) face of goethite is used to illustrate the inner-sphere complex; outer-sphere complexes are not depicted.